Development 129, 2565-2576 (2002)
Printed in Great Britain © The Company of Biologists Limited 2002
DEV5026

Pygopus, a nuclear PHD-finger protein required for Wingless signaling in *Drosophila*

David S. Parker, Jemileh Jemison and Kenneth M. Cadigan*

Department of Molecular, Cellular and Developmental Biology, University of Michigan, Natural Science Building, Ann Arbor, MI 48109, USA
*Author for correspondence (e-mail: cadigan@umich.edu)

Accepted 11 March 2002

SUMMARY

The secreted glycoprotein Wingless (Wg) acts through a conserved signaling pathway to regulate target gene expression. Wg signaling causes nuclear translocation of Armadillo, the fly β-catenin, which then complexes with the DNA-binding protein TCF, enabling it to activate transcription. Though many nuclear factors have been implicated in modulating TCF/Armadillo activity, their importance remains poorly understood. This work describes a ubiquitously expressed protein, called Pygopus, which is required for Wg signaling throughout *Drosophila* development. Pygopus contains a PHD finger at its C terminus, a motif often found in chromatin remodeling factors. Overexpression of *pygopus* also blocks the pathway, consistent with the protein acting in a complex. The *pygopus* mutant phenotype is highly, though not exclusively, specific for Wg signaling. Epistasis experiments indicate that Pygopus acts downstream of Armadillo nuclear import, consistent with the nuclear location of heterologously expressed protein. Our data argue strongly that Pygopus is a new core component of the Wg signaling pathway that acts downstream or at the level of TCF.

Key words: *Drosophila*, Wnt, Wingless, Armadillo, β-catenin, TCF

INTRODUCTION

The *Drosophila* protein Wingless (Wg) is a founding member of the Wnt family of secreted glycoproteins, which are present throughout the animal kingdom. Wnts have been shown to play essential roles in determining many cell fate decisions throughout development in worms, flies, amphibians and mice (Cadigan and Nusse, 1997). In addition, inappropriate activation of Wnt signaling has been linked to several forms of human cancer (Polakis, 2000).

Cells respond to Wg and many vertebrate Wnts by a highly conserved signal transduction cascade that revolves around the Armadillo (Arm; β-catenin in vertebrates) protein (Willert and Nusse, 1998). In the absence of Wg/Wnt signaling, a cytosolic pool of Arm/β-catenin is phosphorylated by a complex of Shaggy/Zeste white 3 (Sgg) (GSK3β in vertebrates), Axin and the adenomatous polyposis coli (APC) protein, then rapidly degraded via the ubiquitination/proteosome pathway (Peifer and Polakis, 2000; Polakis, 2000). Wg/Wnt signaling blocks the activity of the Zw3/GSK3β/Axin/APC complex, resulting in stabilization of Arm/β-catenin (Li et al., 1999; Salic et al., 2000). The stabilized protein then accumulates in the nucleus (Yost et al., 1996), where it forms a complex with members of the TCF/LEF1 (Pangolin – FlyBase) family of HMG group DNA-binding proteins (Molenaar et al., 1996; van de Wetering et al., 1997).

In the absence of Arm, TCF is thought to act as a transcriptional repressor of Wg target genes, through interaction with the transcriptional co-repressor Groucho (Cavallo et al., 1998). In addition, there is good evidence that the ARID domain protein Osa represses Wg target genes by acting in a chromatin remodeling complex that contains the bromodomain protein Brahma (Collins and Treisman, 2000; Treisman et al., 1997). Binding of Arm to TCF somehow blocks the action of these factors, converting TCF from a repressor to an activator (Collins and Treisman, 2000; Korswagen and Clevers, 1999).

In cultured cells, reporter genes with TCF/LEF1-binding sites are highly activated by the transient transfection of β-catenin (Molenaar et al., 1996). β-Catenin/Arm contains transcriptional activation domains both in the N- and C-terminal part of the protein (Cox et al., 1999; Hecht et al., 1999; Hsu et al., 1998; van de Wetering et al., 1997). Several factors have been found to bind to these regions of β-catenin, and to simulate its ability to activate transcription. The CBP/p300 acetyltransferases bind to the C terminus of β-catenin and synergize its transcriptional activity in cultured cells and frog embryos (Hecht et al., 2000; Miyagishi et al., 2000; Sun et al., 2000; Takemaru and Moon, 2000). The DNA helicase Pontin52 (also called TIP49a) binds to the N-terminus of β-catenin and synergizes with it in the reporter gene assay (Bauer et al., 1998). Pontin52 can also bind to the TATA box binding factor TBP, suggesting it links β-catenin/Tcf to the basal transcription complex (Bauer et al., 1998). β-catenin has also been found to bind directly to TBP (Hecht et al., 1999). The *brahma* ortholog Brm1 can also potentiate β-catenin activity in transient

transfection assays (Barker et al., 2001). Thus, β-catenin can promote transcriptional activation from its Tcf anchor in a variety of ways.

The role of the fly homologs of these transcriptional co-activators has also been examined, sometimes with contradictory results. As predicted, *pontin52* genetically acts as a positive regulator of Arm activity (Bauer et al., 2000). However, *nejre* (*nej*), the fly CBP, acts as a negative regulator, in contrast to the data summarized above (Waltzer and Bienz, 1998). With *brahma*, there are reports indicating a negative (Collins and Treisman, 2000) and a positive (Barker et al., 2001) role in regulating Wg targets in the wing. Some of the discrepancies may be explained by these factors acting differently in flies and vertebrates. However, the fly genetics are all based on the examination of partial loss-of-function mutants, often in sensitized backgrounds, or on expression of dominant-negative versions of the proteins. While convenient, these assays can be difficult to interpret clearly.

This report describes the identification of a new factor regulating Wg signaling, which we call Pygopus (Pygo). *pygo* is required for Wg signaling in at least a dozen different readouts in several tissues, suggesting that it is a core component of the pathway. Overexpression of *pygo* also inhibits Wg action, consistent with it acting in a complex. *pygo* is required downstream of Arm nuclear import and encodes a nuclear protein containing a single PHD finger, a zinc-binding motif often found in chromatin remodeling factors (Aasland et al., 1995; Capili et al., 2001; Pascual et al., 2000). Our data are consistent with a model where Pygo is necessary in order for Tcf/Arm to regulate target gene expression.

MATERIALS AND METHODS

Drosophila strains

The P[*GMR-Gal4*] stock used (Freeman, 1996) was obtained from M. Freeman. A P[*UAS-wg*] line was provided by H. Krause. The P[*sev-wg*] transgene has been described previously (Cadigan and Nusse, 1996). These transgenes (all on the second chromosome) were recombined to create the *GMR/wg* and P[*GMR-Gal4*] P[*sev-wg*] stocks used for our EP and secondary screen. The Rorth collection of EP lines (Rorth et al., 1998) were obtained from the BDGP and the Bloomington stock center. The P[*GMR-arm**]^{F36} stock (Freeman and Bienz, 2001) was kindly provided by M. Bienz. The Gal4 driver P[*Ptc-Gal4*] was used and the *dpp-lacZ* line BS3.0 (Blackman et al., 1991) was used to mark *dpp*-expressing cells. The *rod* alleles, X1 and X2 (Scaerou et al., 1999) were obtained from R. Karess and R. Goldberg. An *FRT*^{82B} *Axin* mutant chromosome (Hamada et al., 1999) was provided by N. Tolwinski and E. Wieschaus. *wg*^{CX4} is a molecular null (van den Heuvel et al., 1993).

P[*UAS-pygo*] lines were constructed by cloning the *Bgl*II/*Xho*I fragment of cDNA GH25362 into the pUAST vector (Rorth, 1996). This fragment contains the entire 815 codon ORF and some 5′ and 3′ UTR sequences. The P[*UAS-pygo*] construct was introduced into *w*^{1118} hosts by P-element-mediated transformation. Five independent lines were obtained, one of which gives phenotypes less severe than the others in the GMR/*wg* suppression assay (see Fig. 1). Two of the strongest lines, 1-1 and 1-2 were used for all other experiments.

Deletions of the *pygo* locus were created by imprecise excision of the *EP(3)1076* transposon, using the Δ2-3, Sb chromosome (Robertson et al., 1988). The *EP(3)1076* was outcrossed to *w*^{1118} flies for six generations before isogenization. This removed at least one linked lethal. Approximately 200 white minus males were obtained from dysgenic crosses, and 10 of these had a phenotype more severe than the parental chromosome (which die as pharates). These were characterized using PCR and the relevant PCR bands were sequenced to confirm the nature of each deletion. The alleles *pygo*^{10} and *pygo*^{9} are used in this report.

Clonal analysis

Random clones expressing *pygo* were generated using the P[*Actin>CD2>Gal4*] transgene (Pignoni and Zipursky, 1997). P[*UAS-pygo*] males were crossed to *yw* P[*Actin>CD2>Gal4*]; P[*UAS-GFP*]; P[*HS-Flp*]^{99}/TM6B females. A 60 to 90 minute heat shock 48-72 hours after egg laying (late second and early third larval instar) recombines out the CD2 spacer, generating a clone of Actin/Gal4 cells, which are then dissected and fixed at late third larval instar. The clone is marked with GFP. Unless otherwise indicated, at least 20 clones were examined for each marker.

For clonal analysis of the *pygo*^{10} allele, it was recombined onto a FRT^{82B} chromosome using standard methods (Xu and Rubin, 1993). The *Axin*, *pygo* double mutant was constructed by brute force screening of the male progeny of *FRT*^{82B} *Axin*/*FRT*^{82B} *pygo*^{10} mothers crossed to TM3/TM6 males (the cytological locations of *Axin* and *pygo* are 99C and 100D, respectively). These males were crossed to balancer virgins and sacrificed after progeny were observable. Their genomic DNA was screened for the presence of the *Axin* and *pygo*^{10} alleles using specific PCR primers. Two recombinants were found out of 150 progeny examined. For the rescue experiments of *pygo* embryonic phenotypes described below, a P[*Da-Gal4*] *FRT*^{82B} *pygo*^{10} recombinant was also created.

Clones in the wing imaginal discs were created essentially as described (Xu and Rubin, 1993) with the following modifications. FRT mutant males were crossed to ywP[*HS-Flp*]; *FRT*^{82B} P[*arm-lacZ*] females. The *arm-lacZ* transgene was a generous gift from D. Lessing and R. Nusse. A P[*Ubi-GFP*] was used to mark the clones in Fig. 7G-I. Clones were induced at 48-72 hours after egg laying (second larval instar). Clones in the eye-antennal imaginal discs were induced with P[*Eyeless-Flp*] (Newsome et al., 2000), kindly provided by B. Dickson and marked with *arm-lacZ*. In both wing and eye, the discs were analyzed at late third larval instar. Unless otherwise noted, at least 20 clones were examined for each marker. *pygo*^{10} germline clones were generated using *FRT*^{82B} P[*ovo*^{D}] as described (Chou and Perrimon, 1996) with heat shocks during larval development. Embryos lacking zygotic *pygo* were identified by the absence of *eve-lacZ*.

Whole-mount staining and microscopy

Immunostaining was as described previously (Cadigan and Nusse, 1996). Affinity-purified rabbit anti-Wg antisera (1:60 in discs; 1:20 in embryos) was from R. Nusse, guinea pig anti-Sens (1:50) was from H. Bellen, purified rabbit anti-Dll (1:150) was from G. Panganiban and rat anti-Elav (1:100) was from G. Rubin. Rabbit anti-Eve (1:100) was from Z. Han and R. Bodmer, and rabbit anti-Arm (1:200) was from N. Tolwinski and E. Wieschaus. Mouse monoclonal anti-En supernatant (1:2) was from the University of Iowa Hybridoma Bank, mouse and rabbit anti-β-galactosidase (1:500) from Sigma and Cappel, respectively. Antibody against the human nuclear pore complex protein (NPC) MMS-120P (1:500), which crossreacts with the fly NPC, was purchased from Convance. Cy3- and Cy5-conjugated secondary antibodies were from Jackson Immunochemicals and Alexa Flour 488-conjugated secondaries were from Molecular Probes. All fluorescent pictures were obtained with a Zeiss Axiophot coupled to a Ziess LSM510 confocal apparatus. All images were processed as Abode Photoshop files.

A digoxigenin-labeled *pygo* antisense probe was made using T7 RNA polymerase and *pygo* cDNA GH25362 linearized with *Sac*I. In situ hybridization was performed as described (Cadigan et al., 1998). Embryos were photographed with a Nikon Eclipse800 compound microscope using DIC optics. Cuticles were prepared and

photographed as previously described (Bhanot et al., 1999). Adult fly eyes were frozen overnight and photographed with a Leica M10 microscope.

Cell culture transfections

For the GFP-Pygo chimeric protein, the Pygo ORF was PCR amplified and cloned into the pEGFP vector (Clontech). A fragment containing GFP fused in frame to the N terminus of Pygo was cloned into pAc5.1/V5-His A (Invitrogen), which contains the *Actin 5C* promoter. Sequencing of the chimeric gene revealed a single conservative amino acid substitution (G>V) at amino acid number 732. *Drosophila* S2 cells were obtained from R. Nusse and J. Dixon and cultured in Schneider's *Drosophila* Media plus 10% fetal calf serum (Gibco). These cells were transfected with 1 μg of plasmid/six-well plate using Cellfectin as described by the manufacturer (Gibco) and fixed and immunostained with anti-NPC antibody 40 hours later, as described previously (Bhanot et al., 1996).

RESULTS

A misexpression screen for Wg signaling antagonists in the *Drosophila* eye identifies a novel gene

Drosophila have typical compound insect eyes (Fig. 1A). Misexpression of *wg* using the eye-specific *GMR-Gal4* driver (Freeman, 1996) in combination with *UAS-wg* results in a dramatically reduced eye size (Fig. 1B). This phenotype can be used as the starting point in a misexpression screen for Wg signaling antagonists. If a Wg antagonist such as *Axin* is co-expressed with *wg* in the eye, the small eye phenotype is greatly suppressed (Willert et al., 1999). We used 'EP' P elements, which contain a *Gal4*-dependent promoter (Rorth, 1996), to randomly co-express genes with *wg* in the eye. A collection of 2300 EP lines were crossed to a P[*GMR-Gal4*]/P[*UAS-wg*] (*GMR/wg*) stock and the progeny were scored for suppression of the small eye phenotype.

The initial positives (36) from the screen were crossed to a P[*GMR-Gal4*], P[*sev-wg*] line. P[*sev-wg*] eyes lack interommatidial bristles but are otherwise morphologically normal (Cadigan and Nusse, 1996). Two of the positives suppressed the ability of Wg to inhibit bristles (data not shown), suggesting that they may be bona fide Wg signaling antagonists. One of these lines is inserted adjacent to a known negative regulator of the pathway, *zw3* (*EP(X)1576*). Overexpression of *zw3* is known to suppress Wg signaling (Steitz et al., 1998). The second line (*EP(3)1076*), significantly suppresses the GMR/wg phenotype (Fig. 1C) and corresponds to a novel gene.

The position of EP(3)1076 has been mapped by the Berkeley Drosophila Genome Project (BDGP; http://www.fruitfly.org/index.html) using inverse PCR, which was confirmed by PCR with genomic and EP element-specific primers (data not shown). It is located in a small intron in the 5′ UTR of a gene (BEST:LD21971) we refer to as *pygopus* (*pygo*; Fig. 2A). Northern blot analysis reveals the major isoform of the gene to be approximately 5 kb in length (data not shown). Sequencing of a 4 kb cDNA (GH25362; obtained from the BDGP) confirmed the predicted splice sites (GenBank Accession Number, AY075095). More recent searches have revealed an EST that extends the 5′ end of the transcript (LD18280, Fig. 2A), indicating the *pygo* transcript overlaps the transcript of *rough deal* (*rod*) (Scaerou et al., 1999) by at least 14 bases. This start site gives a transcript length of approximately 4.5 kb, which roughly agrees with the data from northern blots when polyadenylation is taken into consideration.

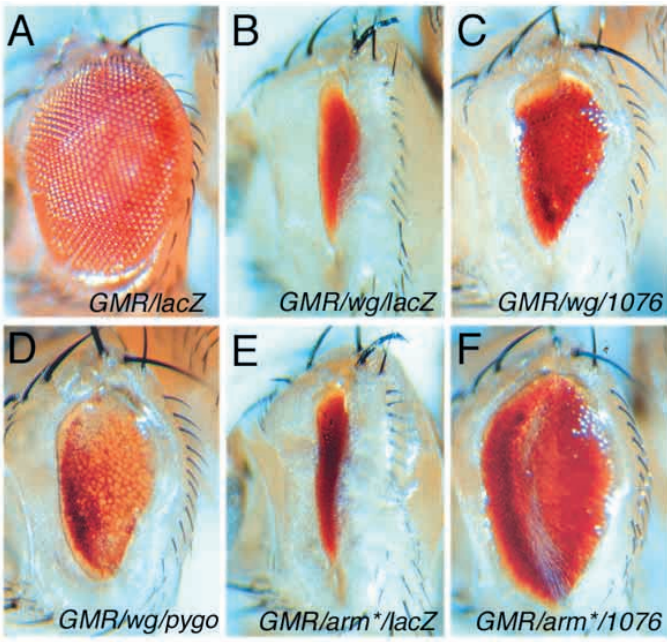

Fig. 1. Expression from *EP(3)1076* or *UAS-pygo* suppresses a Wg signaling-dependant small eye phenotype. Micrographs of adult *Drosophila* eyes all containing P[*GMR-Gal4*] and the following additional transgenes: (A) P[*UAS-lacZ*] (two copies); (B) P[*UAS-wg*], P[*UAS-lacZ*]; (C) P[*UAS-wg*], *EP(3)1076*; (D) P[*UAS-wg*], P[*UAS- pygo*]$^{1-1}$; (E) P[*GMR-arm**], P[*UAS-lacZ*]; (F) P[GMR-arm*], *EP(3)1076*. Expression of *wg* with the *GMR* promoter produces an eye that is severely reduced in size (B) that is prevented by *EP(3)1076* or P[*UAS- pygo*] (C,D). Expression of an activated form of Arm (Freeman and Bienz, 2001) causes a similar reduced eye (E) that is dramatically suppressed by *EP(3)1076* (F) or P[*UAS-pygo*] (data not shown). Unless otherwise noted, each transgene is present in one copy/fly and cultures were reared at 25°C.

The EP(3)1076 transposon is inserted in the proper orientation to misexpress full length *pygo*, and this was confirmed experimentally. First, RT-PCR shows that expression of *pygo*, but not of *rod*, increases dramatically when a heat shock promoter is used to drive *Gal4* expression (data not shown). Second, random clones of cells expressing Gal4 under the control of an *Actin* promoter (Pignoni and Zipursky, 1997) in a *EP(3)1076* background cause a dramatic increase in *pygo* transcript levels (Fig. 2H). Third, and most directly, a P[*UAS-pygo*] transgene strongly suppresses the GMR/wg phenotype (Fig. 1D). These data argue that *pygo* is responsible for the antagonistic effects of *EP1076* on Wg signaling.

The predicted Pygo protein contains 815 amino acids and possesses two recognized motifs, a predicted NLS at the N terminus (residues 39-44) and a PHD domain at the C terminus (residues 747-811; Fig. 2A). The function of PHD domains is unclear. They are zinc finger-binding motifs (Capili et al., 2001; Pascual et al., 2000), and are found in many transcription factors and chromatin remodeling proteins (Aasland et al., 1995).

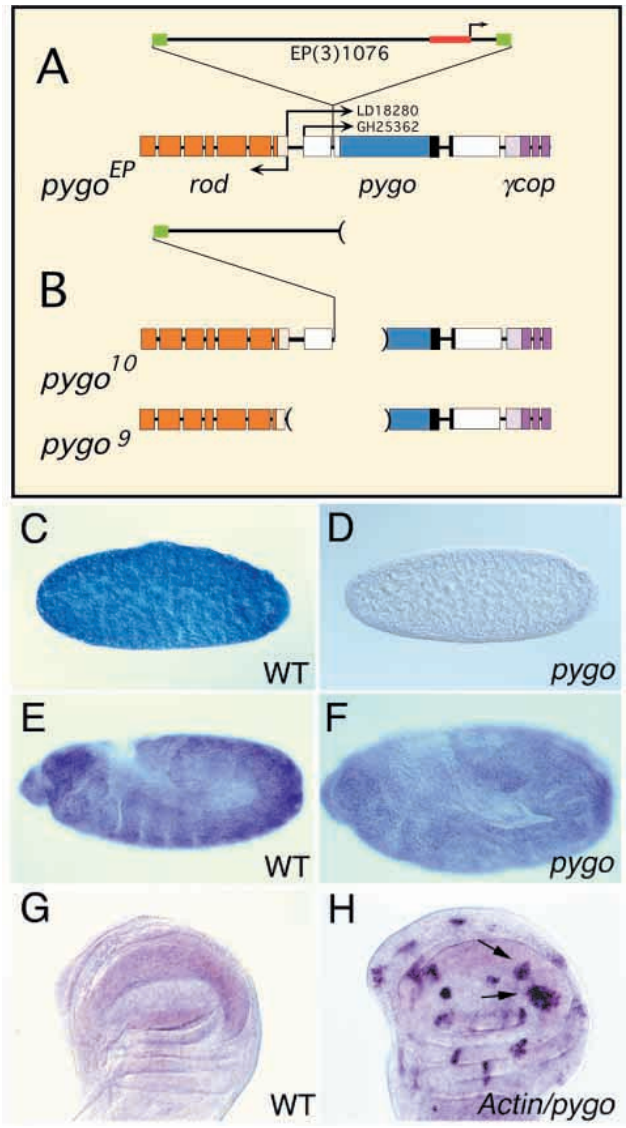

Fig. 2. Cartoon of the *pygo* locus and mutant alleles and *pygo* expression profile. (A) The *pygo* locus with flanking genes rough deal (*rod*) and *γ-cop*. The location and orientation of the *EP(3)1076* transposon is also shown. Besides the Gal4-dependent dominant phenotypes seen with *EP(3)1076*, the transposon also causes a Gal4-independent recessive phenotype (referred to as $pygo^{EP}$). (B) Depiction of two additional *pygo* loss-of-function alleles created by imprecise excision of *EP(3)1076*. $pygo^{10}$ contains half of the transposon and removes the splice acceptor site in the 5′ UTR intron of the *pygo* gene, and the first 295 residues of the Pygo ORF. It does not affect *rod* (see Results). The $pygo^{9}$ mutation extends further upstream of *pygo*, and inactivates *rod* as well. In situ hybridization of embryos (C-F) and wing imaginal discs (G,H) with a probe for *pygo*. Preblastoderm wild-type embryo (C) shows high levels of staining that are absent in $pygo^{10}$ germline clones (D). At stage 10, wild-type embryos (E) show ubiquitous staining at a much lower level than in C (the preparation was allowed to develop much longer). Stage 10 embryos maternally and zygotically mutant for the $pygo^{10}$ allele (F; identified by their altered morphology) presumably indicate the level of background staining under these conditions. Late third instar wing imaginal discs show low levels of ubiquitous signal (G), while discs containing random clones of Gal4-expressing cells (via an actin promoter) in a *EP(3)1076* background show patches of cells (arrows) with much higher levels of *pygo* transcripts (H).

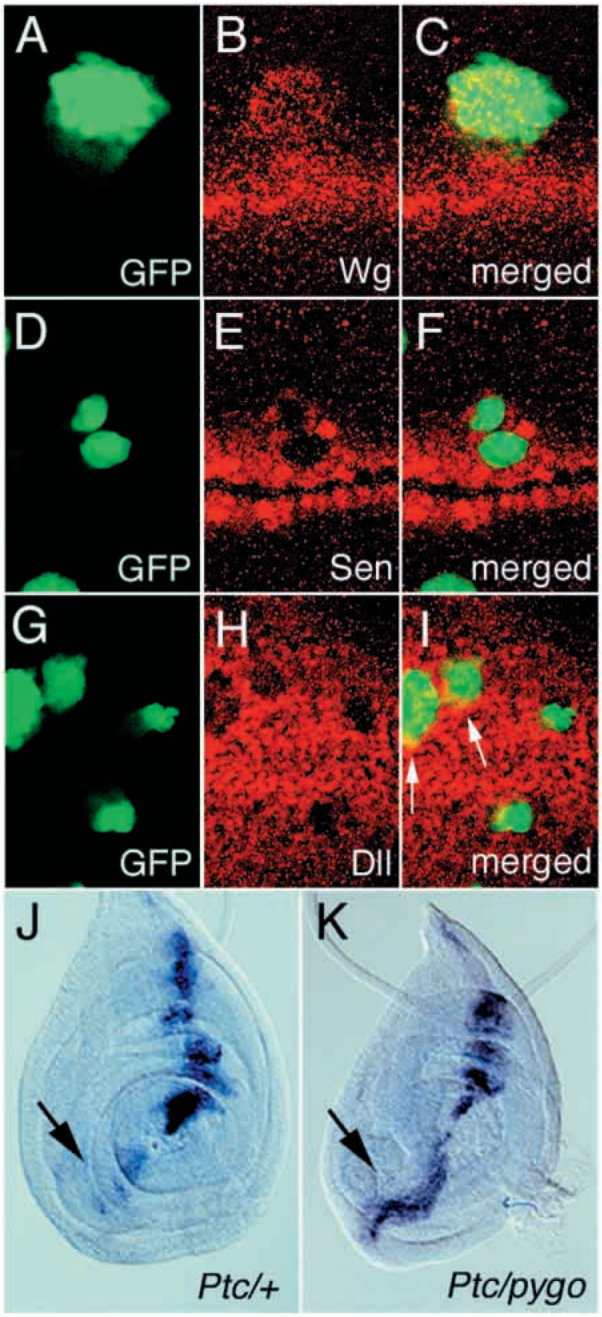

Fig. 3. Overexpression of *pygo* blocks several Wg readouts. (A-I) Confocal images of third instar wing imaginal discs containing random clones of cells overexpressing *pygo*. The clones were marked with GFP (A,D,G) and immunostained with antibodies against Wg (B), Sens (E) or Dll (H). Merged images are shown (C,F,I). Derepression of Wg (B,C) and lack of Sens (E,F; *n*=9) and Dll (H,I) expression were observed, consistent with a block in Wg signaling. The arrows in I indicate boundary regions that are clearly GFP positive (and thus expressing *pygo*) where Dll expression is not reduced. (J,K) Third instar mesothoracic legs of from P[*Ptc-Gal4*]/+ (J) and P[*Ptc-Gal4*]/P[*UAS- pygo*] (K) larva. *dpp* expression is monitored using P[*dpp-lacZ*]. (J) Wild-type pattern, with *lacZ* repressed on the ventral side of the disc (arrow). When *pygo* is overexpressed in this domain, 37% of the legs exhibit complete derepression of *lacZ* on the ventral side (arrow in K indicates a representative of this group); 41% show moderate derepression and 22% show slight or no depression (data not shown; *n*=27).

Database searches reveal that there are potential vertebrate Pygo homologs. An embryonic mouse cDNA (Accession Number, AK011208) and human cDNA (XM_034083) have C-terminal PHD domains similar to that of Pygo (42-47% identity; 63-67% similarity). No other PHD domains in the human or fly genomes are more closely related. There is only one other region of sequence similarity outside this domain, encompassing the predicted NLS of the three genes. Further experiments will be required to determine if these vertebrate proteins function in Wnt signaling.

pygo is ubiquitously expressed

The expression profile of *pygo* in embryos was examined using in situ hybridization. *pygo* is expressed at relatively high levels in pre-blastoderm embryos (Fig. 2C) and this staining is absent in germline clones of *pygo* (Fig. 2D), indicating that it is maternal in origin. *pygo* expression drops rapidly after this early high level, and low levels of signal are observed throughout the embryos for the rest of embryogenesis. For example, at full germband extension, *pygo* expression is at such low levels that visualization of the message requires overstaining, as judged by significant signal in embryos lacking maternal and zygotic *pygo* (compare Fig. 2E,F). We believe that the allele used ($pygo^{10}$) is a molecular null (Fig. 2B), although we cannot rule out that some small amount of aberrant mRNA is produced. In either case, the data indicate a high degree of maternally provided message, followed by a low level of ubiquitous zygotic expression. This continues into larval development, where *pygo* appears to be expressed at low levels in no distinctive pattern (e.g. the wing imaginal disc in Fig. 2G).

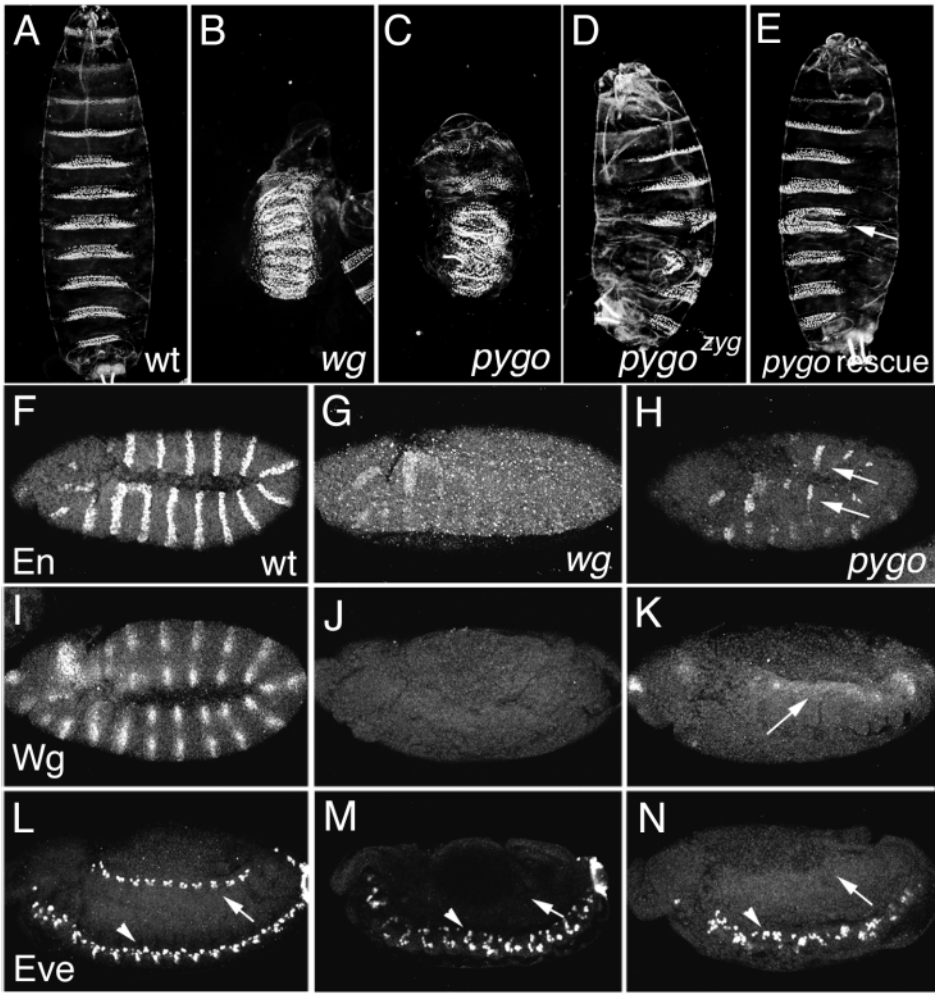

Fig. 4. *pygo* is required for Wg signaling in the embryo. (A-E) Micrographs of cuticles of wild-type (A), wg^{CX4} (B), $pygo^{10}$ maternal/zygotic mutant (C), a $pygo^{10}$ maternal mutant without (D) or with (E) a P[*UAS- pygo*] transgene. The mothers in D,E are heterozygous for P[*Da-Gal4*]. The absence of maternal and zygotic *pygo* results in a denticle lawn similar to that observed in *wg* mutants (compare panel B with C). Paternal rescue of the *pygo* germline clone gives a variable phenotype (see Table 1 for more details), with most cuticles having four to seven abdominal denticles (the one in D has six). Further rescue was observed with the P[*UAS- pygo*] transgene driven by P[*Da-Gal4*] (Table 1), with the example shown in E having seven denticles (arrow indicates the partial fusion of the fourth and fifth abdominal denticles belts). (F-N) Confocal images of wild type (F,I,L), wg^{CX4} (G,J,M) or $pygo^{10}$ maternal/zygotic mutant embryos (H,K,N) stained with antibodies against En (F-H), Wg (I-K) or Eve (L-N). The embryos in F-K are at mid-stage 10 and the ones in L-N are at stage 13. Embryos that lack zygotic *pygo* were unambiguously identified by the absence of *eve-lacZ* staining. Note that at mid-stage 10 (judged by the extent of stomodeum invagination), when wild-type and *wg* mutants are at full germband extension (most clear in F and I), the *pygo* mutants have incomplete extension (clear in H but even more obvious in K). As described in the text, the En and Wg stripes are largely absent at this stage in *pygo* mutants (H,K), though the residual epidermal En expression (arrows) is not observed in *wg* mutants (G). The Eve pericardial expression (arrow in L) is absent in *wg* and *pygo* mutants (arrows in M and N), while Eve expression in the CNS is present (arrowheads).

Overexpression of *pygo* blocks Wg signaling

The suppression of the *GMR/wg* and P[*sev-wg*] phenotypes by *pygo* overexpression is consistent with the notion that high levels of Pygo block Wg signaling. However, the data can also be explained by *pygo* interacting with the targets of Wg in the eye or the promoters driving *wg* expression. To address this, we examined the effect of *pygo* overexpression on Wg readouts in other tissues.

In the third instar wing imaginal discs, *wg* is expressed in a stripe of cells along the dorsoventral border (Couso et al., 1994; Phillips and Whittle, 1993). Wg secreted from these cells is thought to act as a morphogen, regulating both short- and long-range targets (Neumann and Cohen, 1997; Zecca et al., 1996). In addition, Wg signaling refines the distribution of Wg protein by negative autoregulation of *wg* expression (Rulifson et al.,

Table 1. Rescue of *pygo* embryonic mutant phenotypes by ubiquitous expression of *pygo*

P[Da-Gal4], $pygo^{10}$/ $pygo^{10}$ mothers crossed to:	Cuticle phenotypes (% of total)					
			Number of abdominal denticle belts			
	Lawn	Lesser lawn	4/5	6	7	8
+	1	0	67	25	7	0
P[*UAS-pygo*]$^{1\text{-}1}$	0	1	37	35	23	4
$pygo^{10}$/TM3	48	4	35	11	1	1
P[*UAS-pygo*]$^{1\text{-}1}$;$pygo^{10}$/TM3	17	8	31	22	18	4

yw P[*HS-Flp*]/w; P[*Da-Gal4*], FRT^{82B} $pygo^{10}$/FRT^{82B} P[*ovoD*]^{3R} larvae were heat shocked to induce *pygo* germline clones. Half of the eggs of this genotype should contain the P[*Da-Gal4*] transgene. These mothers were crossed to males of the genotypes indicated. Because maternal *pygo* is essential for larval viability, all the progeny were unhatched and thus easily collected for cuticle analysis. The cuticles were divided into six groups: Lawns are similar to the cuticle shown in Fig. 5C; lesser lawns are larger but still have little naked cuticle (it is not clear whether these are maternal/zygotic mutants or the most severe maternal ones). The remaining four classes were scored by the number of abdominal denticle belts (Fig. 5D is a six, while Fig. 5E is a seven), regardless of other aspects of morphology. This rigid grouping underestimates the difference between rescued and non-rescued crosses, but is highly objective. The number of progeny scored for each cross are, in descending order: 88, 279, 135 and 142. Similar results were obtained with P[*UAS-pygo*]$^{1\text{-}2}$ (data not shown).

1996) and downregulation of the Wg receptor Frizzled2 (Fz2) (Cadigan et al., 1998). Thus, the wing imaginal disc offers several readouts to monitor Wg signaling.

Random clones of cells expressing high levels of *pygo* were generated as described (Pignoni and Zipursky, 1997), except that GFP was used to mark the clones (Cadigan et al., 1998). If a clone is positioned in the endogenous *wg* stripe, it blocks Wg expression (data not shown). This is not seen when Wg signaling is inhibited in these cells (Rulifson et al., 1996), indicating that *pygo* overexpression has consequences not related to Wg signaling. However, if the clone is adjacent to the *wg* stripe, then Wg protein is upregulated (Fig. 3A-C), consistent with a block in Wg signaling. The extent of Wg expansion is similar to that observed in clones mutant for *dishevelled* (a positive regulator of Wg signaling), which is due to derepression of Wg synthesis (Rulifson et al., 1996) and increased Wg stability produced by high levels of Fz2 (Cadigan et al., 1998).

To examine targets that are positively regulated by Wg in the wing, we chose the zinc-finger protein Senseless (Sens) and the homeodomain protein Distal-less (Dll). Sens is expressed in the proneural clusters on either side of the dorsoventral border, immediately adjacent to the Wg expression domain (Nolo et al., 2000). Inhibition of Wg signaling with a dominant-negative TCF blocks Sens expression (data not shown), demonstrating that it is a short-range target of Wg action. *pygo*-expressing cells outside the Wg expression domain completely lack Sens expression (Fig. 3D,E,F). The long-range target Dll (Neumann and Cohen, 1997; Zecca et al., 1996) is also always lost in clones overexpressing *pygo* (Fig. 3G-I). For reasons that are not clear, occasionally some expression persists just inside the clonal border (Fig. 3G-I, see arrows).

Finally, we show that *pygo* overexpression causes derepression of *decapentaplegic* (*dpp*) in leg imaginal discs. In the developing leg, *wg* and *dpp* are expressed in wedge-like domains just anterior to the posterior compartment, with *wg* highly enriched in the ventral half and *dpp* in the dorsal part. If Wg signaling is blocked, *dpp* expression becomes derepressed (Brook and Cohen, 1996; Jiang and Struhl, 1996; Theisen et al., 1996). If *pygo* is misexpressed using the *patched-Gal4* driver, which is active in both the *dpp* and *wg* expression domains, then *dpp* expression (as judged by *dpp-lacZ*) is extended into the ventral compartment (compare arrows in Fig. 3J,K). This derepression of *dpp* expression is seen in the vast majority of leg discs examined and is again consistent with *pygo* overexpression antagonizing Wg signaling.

pygo is required for Wg signaling in the embryo

Overexpression of *pygo* clearly results in phenotypes consistent with a block in Wg signaling. However, a more physiologically relevant test of the importance of *pygo* for Wg function is the analysis of *pygo* mutants. Deletions of the *pygo* locus were created via imprecise excision of the *EP(3)1076* transposon. Several deficiencies were generated, the most useful of which is $pygo^{10}$ (Fig. 2B). This deletion removes the splice acceptor of the first intron and the first 295 residues of the Pygo ORF. Therefore, we believe it is null for *pygo* activity. It fully complements a null allele of *rod* (rod^{X2}) (Scaerou et al., 1999), in contrast to $pygo^{9}$, which removes the transcription start site of *rod* (Fig. 2B). Mutants in γ-cop, the gene on the other side of *pygo*, do not exist, so we can not directly test whether $pygo^{10}$ compromises its activity. However, as the 3′UTR of γ-cop and the intergenic region between it and *pygo* are unaffected in $pygo^{10}$, we consider this unlikely. Thus, $pygo^{10}$ is a deletion specific for *pygo*.

$pygo^{10}$ homozygotes (zygotic mutants) have an early pupal lethal phenotype, as do $pygo^{10}$/$pygo^{9}$ transheterozygotes. However, embryos lacking maternal *pygo* failed to hatch, even when zygotic *pygo* is provided from wild-type males. *pygo* mutant embryos were subjected to cuticle analysis. Wild-type embryos have a distinctive patterning of denticles on their ventral cuticle, with each denticle belt arranged in a trapezoidal pattern with intermittent naked cuticle (Fig. 4A). A *wg* mutant does not form naked cuticle and has a characteristic denticle lawn phenotype (Fig. 4B) (Nusslein-Volhard and Wieschaus, 1980). When mothers producing $pygo^{10}$ mutant eggs are crossed with $pygo^{10}$ heterozygotes, two classes of mutant phenotype are observed. Approximately half the cuticles exhibit a denticle lawn extremely similar to *wg* mutants (compare Fig. 4C with 4B). The other half have a reduction in the number of denticle belts, with some denticle fusions (Fig. 4D; Table 1). This phenotypic class was also observed when the fathers were wild type for *pygo* (Table 1), indicating that they are *pygo* maternal mutants. Thus, embryos lacking both maternal and zygotic *pygo* have a cuticle phenotype indicating a loss of Wg signaling.

To confirm that loss of *pygo* activity is responsible for the phenotypes described above, *pygo* mutant phenotypes were

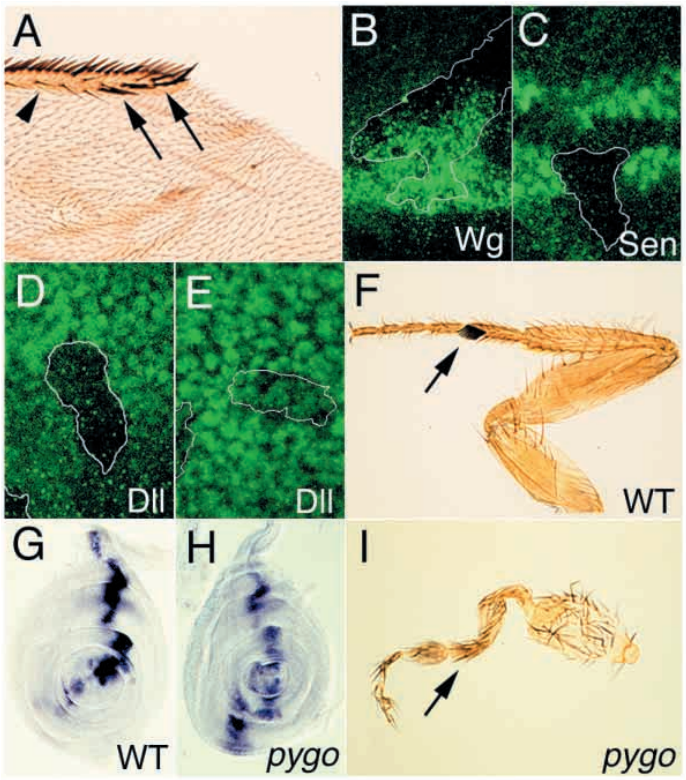

Fig. 5. *pygo* is required for Wg signaling in imaginal discs. (A) Micrograph of an adult wing with a $pygo^{10}$ clone, showing a loss of wing margin and the accompanying bristles. Note that in place of the slender bristles (arrowhead) normally found adjacent to the stout bristles, the tissue next to the clone has ectopic stout bristles (arrows). This is characteristic of a clone that lacks Wg signaling (Rulifson et al., 1996). (B-E) Confocal images of wing imaginal discs stained for Wg (B), Sens (C) and Dll (D,E). Clones of $pygo^{10}$ (marked by the absence of Arm-*lacZ*; not shown, clonal boundaries shown by the white lines). The normal domain of Wg expression is not affected, but Wg expression is derepressed in the adjoining area inside the *pygo* clone (B). Sens is missing in the *pygo* clone (C) and Dll is either completely absent (D), severely reduced (not shown) or modestly affected (E). (F,I) Micrographs of male mesothoracic legs of wild type (F) or a $pygo^{EP}$ homozygote (I). The arrows indicate the position of the sex comb, a row of bristles found on the ventral side of the leg, which is missing in the *pygo* mutant (I). (G,H) Micrographs of third instar leg imaginal discs stained for dpp-*lacZ* in wild type (G) and $pygo^{EP}$ mutants (H). The dorsal marker dpp-*lacZ* is derepressed on the ventral side of the *pygo* mutants.

examined in the presence of P[*UAS-pygo*] and P[*Daughterless-Gal4*] (P[*Da-Gal4*]), which is ubiquitously active during embryogenesis (Wodarz et al., 1995). When *pygo* maternal mutants contain P[*Da-Gal4*] but not P[*UAS-pygo*], 99% of the embryos have a reduction of abdominal denticle belts (Table 1). The cuticle shown in Fig. 4D has six denticle belts; no embryos had all eight. When *pygo* maternal mutants contain P[*Da-Gal4*] and P[*UAS-pygo*], there is a considerable shift of the phenotypic range to the right (Table 1). The cuticle shown in Fig. 4E has seven abdominal belts, and 4% of the progeny had all eight. Keeping in mind that only half of progeny contain P[Da-Gal4] (see Table 1 footnote), the data suggest that ubiquitous expression of *pygo* can significantly rescue the reduction of denticle belts in maternal *pygo* mutants.

P[*Da-Gal4*]/P[*UAS-pygo*] can also significantly rescue *pygo* maternal/zygotic mutants. In control crosses where P[*UAS-pygo*] is omitted, approximately half (52%) of the embryos have a denticle lawn. When the *pygo* transgene is included, only a quarter (25%) of the progeny have a lawn of denticles, which is the predicted result as only half the embryos have zygotic P[*Da-Gal4*]. In fact, the ratio of full to lesser lawns is even better than expected, which could be due to some maternal expression of P[*Da-Gal4*]. There is also an increase in the number of progeny with seven or eight denticle belts (22% versus 2%), which are presumably rescued *pygo* maternal mutants. These results indicate that *pygo* is the gene responsible for the embryonic phenotypes we observe in $pygo^{10}$ mutant embryos.

The *pygo* embryonic phenotype was further characterized using molecular markers. The Engrailed (En) protein is normally expressed in epidermal stripes of single segment periodicity (Fig. 4F). In *wg* mutants, the En stripes are initiated normally but fade from the epidermis by full germband extension (van den Heuvel et al., 1993) (Fig. 4G). In embryos lacking maternal and zygotic *pygo*, the En pattern begins normally but alternating stripes become slightly irregular during germband extension (data not shown). By full germband extension, the En stripes are largely absent but some expression does remain (see arrows Fig. 4H). Wg signaling positively regulates its own striped expression at the same stage, indirectly through maintenance of Hedgehog expression and by a more direct Wg autoregulatory loop (Hooper, 1994). The Wg stripes are normal at early stages (data not shown) but fade at full germband extension in a *pygo* mutant (Fig. 4K). In addition, the dorsal derepression of Wg expression seen in *wg* mutants (van den Heuvel et al., 1993) is also observed in the *pygo* mutants (arrow in Fig. 4K). Both the En and Wg expression patterns in *pygo* maternal/zygotic mutants are consistent with Wg signaling being severely compromised in the absence of *pygo*.

In the mesoderm, Wg is needed for expression of Even skipped (Eve) in a subset of pericardial cells (Wu et al., 1995) (Fig. 4L,M, arrows). In *pygo* null mutants, the pericardial Eve expression is completely absent (Fig. 4N). Eve is still expressed in the CNS in both *wg* and *pygo* mutants, though the pattern is more severely disrupted in *pygo* (compare arrowheads in Fig. 4M and 4N). The Eve-positive RP2 neurons, which are absent in *wg* mutants (Chu-LaGraff and Doe, 1993), are also missing in *pygo* mutants (data not shown), once again consistent with *pygo* being required for Wg signaling.

pygo is required for Wg signaling in imaginal discs

As stated above, $pygo^{10}$ homozygotes and $pygo^{10}/pygo^{9}$ transheterozygotes die around mid-pupation, indicating that maternal *pygo* expression can provide enough activity for viability until this stage. However, the imaginal discs of third instar $pygo^{10}$ homozygotes are severely reduced in size and display abnormal morphology. Therefore, we examined the role of *pygo* in these tissues using mosaic analysis.

Fig. 5A-E show the effects of inducing *pygo* mutant clones in the wing. In the wing imaginal disc, Wg signaling at the dorsoventral boundary of the presumptive wing blade is required for formation of an adult structure known as the wing margin (Couso et al., 1994; Phillips and Whittle, 1993). Wings from flies containing clones of $pygo^{10}$ frequently contain notches, like the one in Fig. 5A, caused by a loss of wing

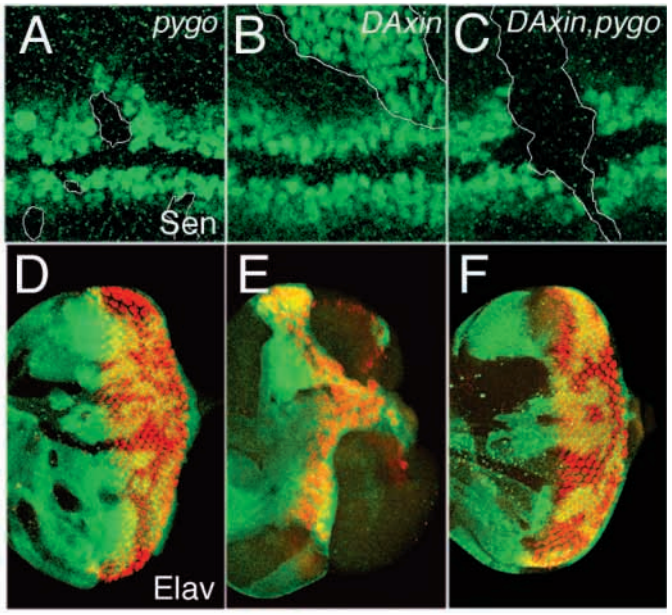

Fig. 6. *pygo* is epistatic to *Axin*. (A-C) Confocal images of wing imaginal discs stained for Sens. Clones (indicated by the white lines) of $pygo^{10}$ (A), *Axin* (B) and *Axin*, $pygo^{10}$ (C) indicate that the double mutant phenotype (loss of Sens in the clone) is identical to *pygo*. (D-F) Confocal images of eye-antennal imaginal discs stained for the photoreceptor marker Elav (red) and clonal marker *lacZ* (green). Clones (indicated by lack of β-gal staining) of $pygo^{10}$ (D), *Axin* (E) and *Axin*, $pygo^{10}$ (F) indicate that the double mutant phenotype (unaffected photoreceptor clusters in the clones) is identical to *pygo*.

margin. To confirm that these notches are due to a loss of Wg signaling, molecular markers were examined at third larval instar as previously determined in *pygo*-overexpressing cells (Fig. 3A-I). Loss of *pygo* causes derepression of Wg adjacent to the stripe and does not affect Wg expression in the stripe (Fig. 5B). *pygo* clones in the wing disc also show a cell autonomous loss of expression of the Wg targets Sens and Dll (Fig. 5C-E). The Sens result was observed with 100% penetrance (n>20). In the case of Dll, all clones had reduced expression, with Dll completely absent 28% of the time (Fig. 5D), a large reduction with 57% frequency (not shown) and a modest reduction in 15% of the clones (Fig. 6E; n=92). Thus, as in the embryo, loss of *pygo* results in a dramatic reduction in several Wg-dependent readouts, though the results with En and Dll suggest that Wg signaling may still occur at a modest level without *pygo*.

In the developing eye, misexpression of *wg* at low levels with the sevenless promoter (P[*sev-wg*]) results in a morphologically normal eye, except that the interommatidial bristles are absent (Cadigan and Nusse, 1996). Expression at higher levels with GMR-*wg* represses the bristles and causes a severe reduction in eye size (Fig. 1B). Clones of $pygo^{10}$ in either misexpression background completely suppress the effects of Wg (data not shown).

Finally, reduction of *pygo* in the leg disc gives phenotypes consistent with loss of Wg signaling. As outlined previously, Wg signaling is required for ventral leg identity, at least in part by repressing the dorsally expressed gene *dpp* (Brook and Cohen, 1996; Jiang and Struhl, 1996; Theisen et al., 1996). To examine the role of *pygo* in the leg, we used a hypomorphic allele. Besides the Gal4-dependent phenotypes observed with *EP(3)1076*, we also found Gal4-independent recessive phenotypes. To avoid confusion, we refer to the *EP(3)1076* allele as $pygo^{EP}$ in this context. $pygo^{EP}$ homozygotes are late pupal lethal, and exhibit several defects in their exoskeleton, including malformed legs (Fig. 5I). The sex comb, a stout row of bristles seen on the ventral side of the first leg in *Drosophila* males (Fig. 5F, arrow) is missing in the $pygo^{EP}$ legs (Fig. 5I, arrow). At the molecular level, the *dpp-lacZ* reporter, which is normally expressed primarily dorsally (Fig. 5G), becomes derepressed ventrally in $pygo^{EP}$ legs (Fig. 5H). Once again, loss of *pygo* results in a phenotype consistent with a loss of Wg signaling. The fact that every Wg readout we examined is *pygo*-dependent suggests that it is a core component of the pathway.

pygo acts downstream of Arm nuclear import

If *pygo* is a core component of Wg signaling in the fly, where does it act in the pathway? We approached this question with epistasis analysis. Initially, this was achieved via overexpression. In the absence of Wnt signaling, β-catenin (and by extension Arm) is believed to be phosphorylated at serine and threonine residues at its N terminus via the GSK3β/Axin/APC complex (Peifer and Polakis, 2000; Polakis, 2000). If these residues are deleted or substituted, β-catenin becomes resistant to degradation (Yost et al., 1996). In flies, these mutant forms of Arm (Arm*) activate Wg signaling independently of Wg (Pai et al., 1997). When placed under the control of the GMR promoter, Arm* causes a small eye phenotype similar to that of GMR-*wg* (Fig. 1E) (Freeman and Bienz, 2001). Co-expression of *pygo* severely suppresses this phenotype (Fig. 1F). This strongly suggests that *pygo* overexpression blocks Wg signaling downstream of Wg-induced Arm stabilization.

To examine the position of *pygo* in the pathway using loss-of-function genetics, we created *Axin*, *pygo* double mutants. In *Axin* mutants, the signaling pathway is constitutively activated because of stabilization of Arm (Hamada et al., 1999; Tolwinski and Wieschaus, 2001; Willert et al., 1999). As found in vertebrate systems, Axin functions in a complex with Sgg to phosphorylate Arm (Willert et al., 1999; Yanagawa et al., 2000). The Wg target gene Sens was used as a readout in wing imaginal discs. As shown before (Fig. 5C), in *pygo* clones, Sens expression adjacent to the dorsal/ventral Wg stripe is lost (Fig. 6A). In *Axin* clones, Sens is activated (Fig. 6B), no matter where in the presumptive wing blade the clones are located (data not shown), as loss of *Axin* constitutively activates Wg signaling (Hamada et al., 1999). In *Axin*, *pygo* double mutant clones, Sens expression was always lost (Fig. 6C). Thus, *pygo* acts downstream of *Axin* in this assay.

Epitasis analysis was also performed in the eye. At the beginning of the third larval instar, a wave of apical constriction of the columnar epithelial cells, called the morphogenetic furrow (MF) sweeps across the presumptive eye from the posterior to the anterior (Wolff and Ready, 1993). Behind the MF, ordered clusters of photoreceptors develop (red stain in Fig. 6D). When Wg signaling is activated in the primordial eye, such as in *Axin* mutant clones, no photoreceptors are specified (Lee and Treisman, 2001). Thus, the eye offers another test of whether *pygo* is epistatic to *Axin*.

Photoreceptor development, as judged by Elav staining,

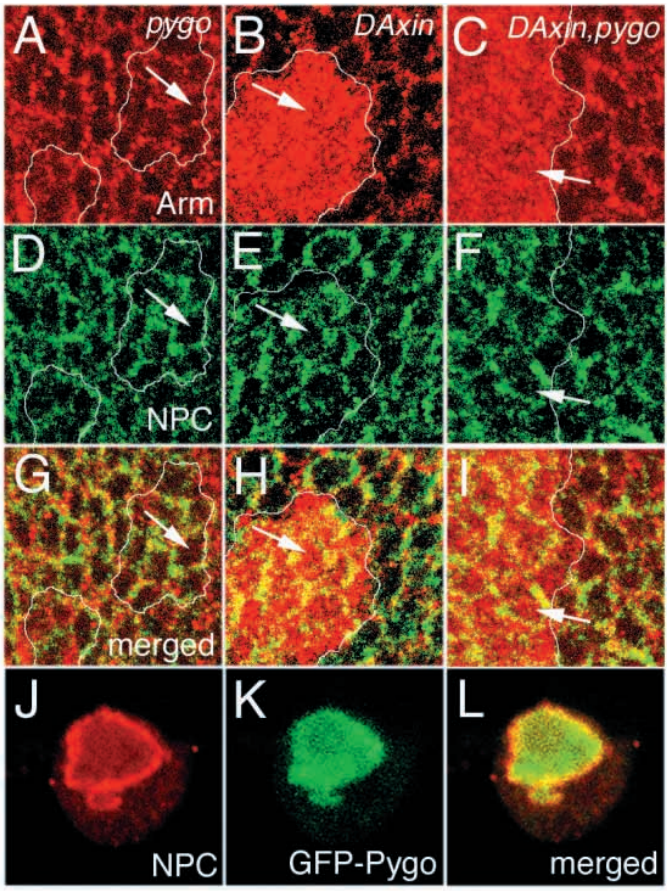

Fig. 7. *pygo* encodes a nuclear protein that acts downstream of Arm nuclear import. (A-I) Confocal images of wing imaginal discs stained for Arm (red) and a NPC antigen (green). Arrows indicate nucleoplasm. Clones (indicated by the white lines) of $pygo^{10}$ (A,D,G), *Axin* (B,E,H) and *Axin*, $pygo^{10}$ (C,F,I) indicate that the double mutant phenotype (high levels of nuclear Arm; see arrows in H,I) is nearly identical to *Axin*. (J-L) Confocal image of a S2 cell transiently transfected with a GFP-Pygo chimeric gene driven by the constitutive *Actin5C* promoter. NPC staining is shown in red and GFP in green. Almost all the GFP signal is found in the nucleus. All images are single optical slices of <1 μm depth.

appears normal in *pygo* mutant cells (Fig. 6D; clones are marked by a lack of green signal). Even at higher magnification, no detectable difference was observed in the photoreceptor clusters between *pygo*-positive and *pygo* mutant cells (data not shown). As previously reported (Lee and Treisman, 2001) clones that lacked *Axin* lack any evidence of photoreceptor development (Fig. 6E). This dramatic phenotype is completely rescued in *Axin*, *pygo* double mutant clones (Fig. 6F), clearly demonstrating that *pygo* is epistatic to *Axin*. This is consistent with the overexpression studies that suggest *pygo* acts downstream of Arm stabilization.

We attempted to extend the epitasis analysis by examining the cuticles of *Axin*, *pygo* germline clones, but despite the fact that many *Axin* or *pygo* germline eggs could be obtained, only a few malformed eggs that were not fertilized were obtained with *Axin*, *pygo* double mutants.

When Wg signaling is activated, Arm is stabilized and translocates to the nucleus. In *Drosophila*, it has proved very difficult to detect nuclear Arm, even in cells receiving high levels of endogenous Wg (Tolwinski and Wieschaus, 2001). However, it has recently been shown that *Axin* maternal and zygotic mutant embryos display high levels of nuclear Arm (Tolwinski and Wieschaus, 2001). Because attempts to make *Axin*, *pygo* germline clones were unsuccessful, clones in the wing disc were generated to investigate Arm levels and localization. In clones of cells lacking *pygo*, Arm is present at low levels at the cell periphery, consistent with its role in adherence junctions (Fig. 7A,D,G) (Willert and Nusse, 1998). In *Axin* clones, Arm protein levels are greatly increased in both the nucleus (Fig. 7B,E,H) and cytoplasm (data not shown). *Axin*, *pygo* double mutant clones also have high levels of cytosolic and nuclear Arm (Fig. 7C,F,I), though the nuclear levels of Arm appear slightly less than in Axin clones (compare Fig. 7B with 7C). We interpret these data to mean that Arm is still stabilized in the absence of *pygo* (as would be expected if *pygo* acts downstream of *Axin*) and that, for the most part, *pygo* is not required for Arm nuclear import.

Consistent with these data, a GFP-Pygo fusion protein localizes to the nucleus in a *Drosophila* cell line. Compare Fig. 7J,K,L, which show GFP-Pygo localization in relation to the nuclear membrane and indicate that, under these conditions, the vast majority of Pygo is in the nucleus. Thus *pygo* acts genetically downstream of Arm stability and nuclear import, consistent with the nuclear localization of the Pygo fusion protein.

DISCUSSION

Pygo is a core component of the Wg signaling pathway

In this study, a total of twelve distinct readouts of Wg signaling from embryos and leg, wing and eye imaginal discs were found to be significantly (two readouts) or completely (ten readouts) blocked in cells lacking *pygo* (Figs 4-6). The effects of *pygo* loss in clones were completely cell autonomous for Wg and Sens expression in the wing (Fig. 5B,C). In addition, *pygo* transcripts are ubiquitously expressed at low levels throughout embryonic and larval tissues (Fig. 2C,E,G). It is formally possible that *pygo* acts to produce a factor that is required for Wg signaling or acts in parallel to the pathway. However, the fact that *pygo* is required for Wg action in so many contexts favors a model where Pygo acts directly in the signal transduction cascade of cells that receive Wg.

In the case of the embryonic En stripes (Fig. 4H) and Dll expression in the wing blade primordia (Fig. 5E), the loss of *pygo* activity resulted in a less severe effect than that observed in *wg* or Wg signaling component mutants (Neumann and Cohen, 1997; van den Heuvel et al., 1993; Zecca et al., 1996). The current model of Wg action in the wing, where Wg is thought to act as a morphogen, postulates that the *Dll* promoter requires a low level of Wg signaling for its activation (Neumann and Cohen, 1997; Zecca et al., 1996). Perhaps loss of *pygo* does not completely abolish Wg signaling, so that there is still some activation of *Dll* and *en*. Alternatively, there could be a redundant factor that can partially replace *pygo*, or specific promoters are less sensitive to loss of *pygo* than others. However, the ability of *pygo* mutants to block the high levels of signaling induced by loss of *Axin* (Fig. 6A-F), argues that

many targets absolutely require *pygo* even when Wg signaling is greatly elevated.

Mechanism of Pygo action

Where does Pygo act in the Wg signaling pathway? Our experiments indicate that *pygo* acts downstream of *Axin* (Fig. 6), an activated form of *Arm* (Fig. 1F) and *Arm* nuclear import (Fig. 7A-I). Consistent with this, a tagged form of Pygo is nuclear (Fig. 7J-L). Taken together these data strongly suggests that Pygo acts in the nucleus, probably at the transcriptional level.

How *pygo* influences transcription of Wg target genes in the nucleus could occur in several ways. Simple explanations include that *pygo* could simply be required for the interaction of Arm with TCF, or for TCF to bind to DNA. However, the fact that Arm still accumulates to high levels in the nuclei of *Axin*, *pygo* mutant cells (Fig. 7C,F,I) may indicate that the Arm/TCF/DNA complex still forms in the absence of *pygo*. It has been shown that expression of a dominant-negative version of TCF (which lacks the Arm-binding domain but retains its ability to bind DNA) prevents Arm nuclear accumulation (Tolwinski and Weischaus, 2001). This supports the idea that TCF acts as a nuclear tether for stabilized Arm. Using this line of reasoning, Arm is still found in the nuclei of *Axin*, *pygo* mutant cells because it is still bound by TCF, which is still localized properly on the DNA. It should be noted that we do see a subtle reduction in nuclear Arm accumulation in *Axin*, *pygo* versus *Axin* mutant cells (compare Fig. 7C with 7B). However, the small difference suggests that this effect by be indirect.

Another line of evidence suggesting that *pygo* is not required for TCF to bind to DNA comes from a detailed analysis of the pericardial enhancer of the *eve* gene. Eve expression in the pericardial cells is absent in *wg* and *pygo* mutants (Fig. 4M,N). Mutation of a single high-affinity site in the pericardial enhancer significantly reduces expression (Halfon et al., 2000). However, mutation of all the sites bound by TCF in vitro revealed a depression of the enhancer throughout the dorsal mesoderm, suggesting that in the absence of Wg signaling, Tcf represses the *eve* pericardial enhancer (Knirr and Frasch, 2001). As no such derepression of Eve expression was observed in *pygo* mutants (Fig. 4N), this suggests that TCF can bind to the *eve* enhancer and repress transcription in the absence of *pygo*.

If Pygo does not promote DNA binding of TCF or formation of the Arm/TCF/DNA complex, what might it be doing? Pygo could help positive factors like Pontin52 (Bauer et al., 2000) to complex with Arm/TCF, or it could normally prevent negative factors like Groucho (Cavallo et al., 1998) or Osa (Collins and Treisman, 2000) from localizing to Wg target genes. In addition, there are a multitude of additional negative regulators of TCF activity identified in vertebrates (see Hecht and Kemler, 2000 for a noncomprehensive list). Pygo could negatively regulate any of these factors.

While the above possibilities must be addressed, the presence of the PHD domain in the Pygo protein suggests another model. PHD domains are often found in chromatin remodeling factors (Aasland et al., 1995). These complexes are thought to alter chromatin structure to allow activation or repression of specific genes (Mahmoudi and Verrijzer, 2001; Urnov and Wolffe, 2001). The PHD domain is a zinc-binding domain that does not bind DNA, and is thought to be involved in protein-protein interactions (Capili et al., 2001; Linder et al., 2000; O'Connell et al., 2001). Therefore, it is possible that *pygo* is a member of such a chromatin remodeling complex.

The finding that overexpression of full-length Pygo inhibits Wg signaling is consistent with Pygo acting in a multisubunit complex. For example, a heterotrimeric complex consisting of A/Pygo/B could be disrupted by an abundance of Pygo, shifting the equilibrium to A/Pygo and B/Pygo heterodimers. While this is speculation, examples of similar situations are known for histone octomers (Meeks-Wagner and Hartwell, 1986), Apterous/Chip tetramers (Fernandez-Funez et al., 1998) and cytoskeletal complexes (Stokes et al., 2000).

Specificity of Pygo action

The genetic case for the importance of Pygo in Wg signaling is so convincing because we could directly remove *pygo* in many tissues and see phenotypes specifically related to Wg signaling. This is in contrast to other Wg transcriptional regulators like Groucho, Osa and Nejire, where complete loss of activity results in pleiotropic phenotypes (Akimaru et al., 1997; Cavallo et al., 1998; Paroush et al., 1994; Treisman et al., 1997; Waltzer and Bienz, 1998). For these factors, and for Pontin52 and Reptin52 (Bauer et al., 2000), the genetic evidence was limited to partial reduction of gene activity, often in a background where Wg signaling was already attenuated. Because of this, it is impossible to explore fully the importance of these genes in the regulation of Wg targets. Even in the case of TCF, its inconvenient location on the fourth chromosome has prevented a detailed genetic analysis (i.e. germline and somatic clonal analysis), though very specific embryonic phenotypes are obtained with zygotic mutants (Brunner et al., 1997; van de Wetering et al., 1997). In this regard, *pygo* is most similar to *arm*, whose loss-of-function phenotype has been carefully analyzed in many contexts (Cadigan and Nusse, 1996; Neumann and Cohen, 1997; Peifer et al., 1991; van den Heuvel et al., 1993).

Does *pygo* have any functions other than regulation of Wg signaling? The phenotypes obtained in clonal analysis in the wing and eye suggests that *pygo* is highly specific for Wg signaling in these tissues. The fact that clones of *pygo* in the eye have no detectable defects in morphogenetic furrow progression and photoreceptor recruitment (Fig. 6D,F) or in the morphology of the adult eye (data not shown) is especially impressive. Eye development requires a cadre of transcription factors, including Eyeless, Sine oculis and Eyes absent, that act in concert with Hedgehog, Dpp, Notch and Ras signaling act to specify eye identity in the growing eye-antennal disc (Kumar and Moses, 2001). However, while the data in the embryo suggests that *pygo* primarily affects Wg signaling (Fig. 4), it is also required for non Wg-dependent processes. For example, when *pygo* germline clones are zygotically rescued, they have cuticles that appear, at least on a superficial level, to be of the pair-rule class (Fig. 4D). Such phenotypes are not seen in *wg*, *dsh* or *arm* mutant embryos (Peifer et al., 1991; van den Heuvel et al., 1993). Pygo is not a pair-rule mutant in the classical sense, as even in the complete absence of *pygo* En and Wg stripes are normal at cellular blastoderm. Rather, the decrease in alternative En stripes begins during germband extension (data not shown). *pygo* maternal/zygotic mutants also have morphological abnormalities not seen in *wg* mutants, such as

incomplete germ-band extension (Fig. 4H,K) and less organized epithelium (data not shown), another indication of a wider role for *pygo*. Thus, while *pygo* is highly dedicated to Wg signaling, it clearly has other roles as well.

The authors thank everyone mentioned in Materials and Methods for providing fly stocks and antisera. Special thanks to T. Laverty from the BDGP for coordinating the shipment of EP lines. Thanks also to R. Cohen and A. Singal for help with maintaining the EP lines and performing the screen. S. Klinedinst participated in the initial characterization of *EP(3)1076*, and R. Angeles and A. Singal contributed to the cell transfection experiments. H. Lin confirmed that Sens expression was inhibited by dominant-negative Tcf. Thanks to W. Lockwood and R. Bodmer for helpful discussions and to R. Nusse for encouragement and inspiration. D. S. P. and J. J. were supported by the Genetics Training Grant of the University of Michigan. This work was supported by a Rackham Grant from the University of Michigan and NIH grant RO1 GM59846 to K. M. C.

REFERENCES

Aasland, R., Gibson, T. J. and Stewart, A. F. (1995). The PHD finger: implications for chromatin-mediated transcriptional regulation. *Trends Biochem. Sci.* **20**, 56-59.

Akimaru, H., Hou, D. X. and Ishii, S. (1997). Drosophila CBP is required for dorsal-dependent twist gene expression. *Nat. Genet.* **17**, 211-214.

Barker, N., Hurlstone, A., Musisi, H., Miles, A., Bienz, M. and Clevers, H. (2001). The chromatin remodelling factor Brg-1 interacts with beta-catenin to promote target gene activation. *EMBO J.* **20**, 4935-4943.

Bauer, A., Huber, O. and Kemler, R. (1998). Pontin52, an interaction partner of beta-catenin, binds to the TATA box binding protein. *Proc. Natl. Acad. Sci. USA* **95**, 14787-14792.

Bauer, A., Chauvet, S., Huber, O., Usseglio, F., Rothbacher, U., Aragnol, D., Kemler, R. and Pradel, J. (2000). Pontin52 and reptin52 function as antagonistic regulators of beta- catenin signalling activity. *EMBO J.* **19**, 6121-6130.

Bhanot, P., Brink, M., Samos, C. H., Hsieh, J. C., Wang, Y., Macke, J. P., Andrew, D., Nathans, J. and Nusse, R. (1996). A new member of the frizzled family from Drosophila functions as a Wingless receptor. *Nature* **382**, 225-230.

Bhanot, P., Fish, M., Jemison, J. A., Nusse, R., Nathans, J. and Cadigan, K. M. (1999). Frizzled and Dfrizzled-2 function as redundant receptors for Wingless during Drosophila embryonic development. *Development* **126**, 4175-4186.

Blackman, R. K., Sanicola, M., Raftery, L. A., Gillevet, T. and Gelbart, W. M. (1991). An extensive 3′ cis-regulatory region directs the imaginal disk expression of decapentaplegic, a member of the TGF-beta family in Drosophila. *Development* **111**, 657-666.

Brook, W. J. and Cohen, S. M. (1996). Antagonistic interactions between wingless and decapentaplegic responsible for dorsal-ventral pattern in the Drosophila Leg. *Science* **273**, 1373-1377.

Brunner, E., Peter, O., Schweizer, L. and Basler, K. (1997). pangolin encodes a Lef-1 homologue that acts downstream of Armadillo to transduce the Wingless signal in Drosophila. *Nature* **385**, 829-833.

Cadigan, K. M. and Nusse, R. (1996). *wingless* signaling in the *Drosophila* eye and embryonic epidermis. *Development* **122**, 2801-2812.

Cadigan, K. M. and Nusse, R. (1997). Wnt signaling: a common theme in animal development. *Genes Dev.* **11**, 3286-3305.

Cadigan, K. M., Fish, M. P., Rulifson, E. J. and Nusse, R. (1998). Wingless repression of Drosophila frizzled 2 expression shapes the Wingless morphogen gradient in the wing. *Cell* **93**, 767-777.

Capili, A. D., Schultz, D. C., Rauscher, I. F. and Borden, K. L. (2001). Solution structure of the PHD domain from the KAP-1 corepressor: structural determinants for PHD, RING and LIM zinc-binding domains. *EMBO J.* **20**, 165-177.

Cavallo, R. A., Cox, R. T., Moline, M. M., Roose, J., Polevoy, G. A., Clevers, H., Peifer, M. and Bejsovec, A. (1998). Drosophila Tcf and Groucho interact to repress Wingless signalling activity. *Nature* **395**, 604-608.

Chou, T. B. and Perrimon, N. (1996). The autosomal FLP-DFS technique for generating germline mosaics in Drosophila melanogaster. *Genetics* **144**, 1673-1679.

Chu-LaGraff, Q. and Doe, C. Q. (1993). Neuroblast specification and formation regulated by wingless in the Drosophila CNS. *Science* **261**, 1594-1597.

Collins, R. T. and Treisman, J. E. (2000). Osa-containing Brahma chromatin remodeling complexes are required for the repression of wingless target genes. *Genes Dev.* **14**, 3140-3152.

Couso, J. P., Bishop, S. A. and Martinez Arias, A. (1994). The wingless signalling pathway and the patterning of the wing margin in Drosophila. *Development* **120**, 621-636.

Cox, R. T., Pai, L. M., Kirkpatrick, C., Stein, J. and Peifer, M. (1999). Roles of the C terminus of Armadillo in Wingless signaling in Drosophila. *Genetics* **153**, 319-332.

Fernandez-Funez, P., Lu, C. H., Rincon-Limas, D. E., Garcia-Bellido, A. and Botas, J. (1998). The relative expression amounts of apterous and its co-factor dLdb/Chip are critical for dorso-ventral compartmentalization in the Drosophila wing. *EMBO J.* **17**, 6846-6853.

Freeman, M. (1996). Reiterative use of the EGF receptor triggers differentiation of all cell types in the Drosophila eye. *Cell* **87**, 651-660.

Freeman, M. and Bienz, M. (2001). EGF receptor/Rolled MAP kinase signalling protects cells against activated Armadillo in the Drosophila eye. *EMBO Rep.* **2**, 157-162.

Halfon, M. S., Carmena, A., Gisselbrecht, S., Sackerson, C. M., Jimenez, F., Baylies, M. K. and Michelson, A. M. (2000). Ras pathway specificity is determined by the integration of multiple signal-activated and tissue-restricted transcription factors. *Cell* **103**, 63-74.

Hamada, F., Tomoyasu, Y., Takatsu, Y., Nakamura, M., Nagai, S., Suzuki, A., Fujita, F., Shibuya, H., Toyoshima, K., Ueno, N. et al. (1999). Negative regulation of Wingless signaling by D-axin, a Drosophila homolog of axin. *Science* **283**, 1739-1742.

Hecht, A., Litterst, C. M., Huber, O. and Kemler, R. (1999). Functional characterization of multiple transactivating elements in beta-catenin, some of which interact with the TATA-binding protein in vitro. *J. Biol. Chem.* **274**, 18017-18025.

Hecht, A., Vleminckx, K., Stemmler, M. P., van Roy, F. and Kemler, R. (2000). The p300/CBP acetyltransferases function as transcriptional coactivators of beta-catenin in vertebrates. *EMBO J.* **19**, 1839-1850.

Hooper, J. E. (1994). Distinct pathways for autocrine and paracrine Wingless signalling in Drosophila embryos. *Nature* **372**, 461-464.

Hsu, S. C., Galceran, J. and Grosschedl, R. (1998). Modulation of transcriptional regulation by LEF-1 in response to Wnt-1 signaling and association with beta-catenin. *Mol. Cell. Biol.* **18**, 4807-4818.

Jiang, J. and Struhl, G. (1996). Complementary and mutually exclusive activities of decapentaplegic and wingless organize axial patterning during Drosophila leg development. *Cell* **86**, 401-409.

Knirr, S. and Frasch, M. (2001). Molecular integration of inductive and mesoderm-intrinsic inputs governs even-skipped enhancer activity in a subset of pericardial and dorsal muscle progenitors. *Dev. Biol.* **238**, 13-26.

Korswagen, H. C. and Clevers, H. C. (1999). Activation and repression of wingless/Wnt target genes by the TCF/LEF-1 family of transcription factors. *Cold Spring Harb. Symp. Quant. Biol.* **64**, 141-147.

Kumar, J. P. and Moses, K. (2001). Eye specification in Drosophila: perspectives and implications. *Semin. Cell Dev. Biol.* **12**, 469-474.

Lee, J. D. and Treisman, J. E. (2001). The role of Wingless signaling in establishing the anteroposterior and dorsoventral axes of the eye disc. *Development* **128**, 1519-1529.

Li, L., Yuan, H., Weaver, C. D., Mao, J., Farr, G. H., 3rd, Sussman, D. J., Jonkers, J., Kimelman, D. and Wu, D. (1999). Axin and Frat1 interact with dvl and GSK, bridging Dvl to GSK in Wnt-mediated regulation of LEF-1. *EMBO J.* **18**, 4233-4240.

Linder, B., Newman, R., Jones, L. K., Debernardi, S., Young, B. D., Freemont, P., Verrijzer, C. P. and Saha, V. (2000). Biochemical analyses of the AF10 protein: the extended LAP/PHD-finger mediates oligomerisation. *J. Mol. Biol.* **299**, 369-378.

Mahmoudi, T. and Verrijzer, C. P. (2001). Chromatin silencing and activation by Polycomb and trithorax group proteins. *Oncogene* **20**, 3055-3066.

Meeks-Wagner, D. and Hartwell, L. H. (1986). Normal stoichiometry of histone dimer sets is necessary for high fidelity of mitotic chromosome transmission. *Cell* **44**, 43-52.

Miyagishi, M., Fujii, R., Hatta, M., Yoshida, E., Araya, N., Nagafuchi, A., Ishihara, S., Nakajima, T. and Fukamizu, A. (2000). Regulation of Lef-

mediated transcription and p53-dependent pathway by associating beta-catenin with CBP/p300. *J. Biol. Chem.* **275**, 35170-35175.

Molenaar, M., van de Wetering, M., Oosterwegel, M., Peterson-Maduro, J., Godsave, S., Korinek, V., Roose, J., Destree, O. and Clevers, H. (1996). XTcf-3 transcription factor mediates beta-catenin-induced axis formation in Xenopus embryos. *Cell* **86**, 391-399.

Neumann, C. J. and Cohen, S. M. (1997). Long-range action of Wingless organizes the dorsal-ventral axis of the Drosophila wing. *Development* **124**, 871-880.

Newsome, T. P., Schmidt, S., Dietzl, G., Keleman, K., Asling, B., Debant, A. and Dickson, B. J. (2000). Trio combines with dock to regulate Pak activity during photoreceptor axon pathfinding in Drosophila. *Cell* **101**, 283-294.

Nolo, R., Abbott, L. A. and Bellen, H. J. (2000). Senseless, a Zn finger transcription factor, is necessary and sufficient for sensory organ development in Drosophila. *Cell* **102**, 349-362.

Nusslein-Volhard, C. and Wieschaus, E. (1980). Mutations affecting segment number and polarity in Drosophila. *Nature* **287**, 795-801.

O'Connell, S., Wang, L., Robert, S., Jones, C. A., Saint, R. and Jones, R. S. (2001). Polycomblike PHD fingers mediate conserved interaction with Enhancer of Zeste protein. *J. Biol. Chem.* **276**, 43065-43073.

Pai, L. M., Orsulic, S., Bejsovec, A. and Peifer, M. (1997). Negative regulation of Armadillo, a Wingless effector in *Drosophila*. *Development* **124**, 2255-2266.

Paroush, Z., Finley, R. L., Jr, Kidd, T., Wainwright, S. M., Ingham, P. W., Brent, R. and Ish-Horowicz, D. (1994). Groucho is required for Drosophila neurogenesis, segmentation, and sex determination and interacts directly with hairy-related bHLH proteins. *Cell* **79**, 805-815.

Pascual, J., Martinez-Yamout, M., Dyson, H. J. and Wright, P. E. (2000). Structure of the PHD zinc finger from human Williams-Beuren syndrome transcription factor. *J. Mol. Biol.* **304**, 723-729.

Peifer, M. and Polakis, P. (2000). Wnt signaling in oncogenesis and embryogenesis – a look outside the nucleus. *Science* **287**, 1606-1609.

Peifer, M., Rauskolb, C., Williams, M., Riggleman, B. and Wieschaus, E. (1991). The segment polarity gene armadillo interacts with the wingless signaling pathway in both embryonic and adult pattern formation. *Development* **111**, 1029-1043.

Phillips, R. G. and Whittle, J. R. (1993). wingless expression mediates determination of peripheral nervous system elements in late stages of Drosophila wing disc development. *Development* **118**, 427-438.

Pignoni, F. and Zipursky, S. L. (1997). Induction of Drosophila eye development by decapentaplegic. *Development* **124**, 271-278.

Polakis, P. (2000). Wnt signaling and cancer. *Genes Dev.* **14**, 1837-1851.

Robertson, H. M., Preston, C. R., Phillis, R. W., Johnson-Schlitz, D. M., Benz, W. K. and Engels, W. R. (1988). A stable genomic source of P element transposase in Drosophila melanogaster. *Genetics* **118**, 461-470.

Rorth, P. (1996). A modular misexpression screen in Drosophila detecting tissue-specific phenotypes. *Proc. Natl. Acad. Sci. USA* **93**, 12418-12422.

Rorth, P., Szabo, K., Bailey, A., Laverty, T., Rehm, J., Rubin, G. M., Weigmann, K., Milan, M., Benes, V., Ansorge, W. et al. (1998). Systematic gain-of-function genetics in Drosophila. *Development* **125**, 1049-1057.

Rulifson, E. J., Micchelli, C. A., Axelrod, J. D., Perrimon, N. and Blair, S. S. (1996). wingless refines its own expression domain on the Drosophila wing margin. *Nature* **384**, 72-74.

Salic, A., Lee, E., Mayer, L. and Kirschner, M. W. (2000). Control of beta-catenin stability: reconstitution of the cytoplasmic steps of the wnt pathway in Xenopus egg extracts. *Mol. Cell* **5**, 523-532.

Scaerou, F., Aguilera, I., Saunders, R., Kane, N., Blottiere, L. and Karess, R. (1999). The rough deal protein is a new kinetochore component required for accurate chromosome segregation in Drosophila. *J. Cell Sci.* **112**, 3757-3768.

Steitz, M. C., Wickenheisser, J. K. and Siegfried, E. (1998). Overexpression of zeste white 3 blocks wingless signaling in the Drosophila embryonic midgut. *Dev. Biol.* **197**, 218-233.

Stokes, K. D., McAndrew, R. S., Figueroa, R., Vitha, S. and Osteryoung, K. W. (2000). Chloroplast division and morphology are differentially affected by overexpression of FtsZ1 and FtsZ2 genes in Arabidopsis. *Plant Physiol.* **124**, 1668-1677.

Sun, Y., Kolligs, F. T., Hottiger, M. O., Mosavin, R., Fearon, E. R. and Nabel, G. J. (2000). Regulation of β-catenin transformation by the p300 transcriptional coactivator. *Proc. Natl. Acad. Sci. USA* **97**, 12613-12618.

Takemaru, K. I. and Moon, R. T. (2000). The transcriptional coactivator CBP interacts with beta-catenin to activate gene expression. *J. Cell Biol.* **149**, 249-254.

Theisen, H., Haerry, T. E., O'Connor, M. B. and Marsh, J. L. (1996). Developmental territories created by mutual antagonism between Wingless and Decapentaplegic. *Development* **122**, 3939-3948.

Tolwinski, N. S. and Wieschaus, E. (2001). Armadillo nuclear import is regulated by cytoplasmic anchor Axin and nuclear anchor dTCF/Pan. *Development* **128**, 2107-2117.

Treisman, J. E., Luk, A., Rubin, G. M. and Heberlein, U. (1997). eyelid antagonizes wingless signaling during Drosophila development and has homology to the Bright family of DNA-binding proteins. *Genes Dev.* **11**, 1949-1962.

Urnov, F. D. and Wolffe, A. P. (2001). Chromatin remodeling and transcriptional activation: the cast (in order of appearance). *Oncogene* **20**, 2991-3006.

van de Wetering, M., Cavallo, R., Dooijes, D., van Beest, M., van Es, J., Loureiro, J., Ypma, A., Hursh, D., Jones, T., Bejsovec, A. et al. (1997). Armadillo coactivates transcription driven by the product of the Drosophila segment polarity gene dTCF. *Cell* **88**, 789-799.

van den Heuvel, M., Klingensmith, J., Perrimon, N. and Nusse, R. (1993). Cell patterning in the Drosophila segment: engrailed and wingless antigen distributions in segment polarity mutant embryos. *Development* **Suppl.**, 105-114.

Waltzer, L. and Bienz, M. (1998). Drosophila CBP represses the transcription factor TCF to antagonize Wingless signalling. *Nature* **395**, 521-525.

Willert, K., Logan, C. Y., Arora, A., Fish, M. and Nusse, R. (1999). A Drosophila Axin homolog, Daxin, inhibits Wnt signaling. *Development* **126**, 4165-4173.

Willert, K. and Nusse, R. (1998). Beta-catenin: a key mediator of Wnt signaling. *Curr. Opin. Genet. Dev.* **8**, 95-102.

Wodarz, A., Hinz, U., Engelbert, M. and Knust, E. (1995). Expression of crumbs confers apical character on plasma membrane domains of ectodermal epithelia of Drosophila. *Cell* **82**, 67-76.

Wolff, T. and Ready, D. F. (1993). Pattern formation in the Drosophila retina. In *The Development of* Drosophila melanogaster, Vol. II (ed. M. A. Bate and A. Martinez Arias), pp. 1277-1326. New York: Cold Spring Harbor Laboratory Press.

Wu, X., Golden, K. and Bodmer, R. (1995). Heart development in Drosophila requires the segment polarity gene wingless. *Dev. Biol.* **169**, 619-628.

Xu, T. and Rubin, G. M. (1993). Analysis of genetic mosaics in developing and adult Drosophila tissues. *Development* **117**, 1223-1237.

Yanagawa, S., Lee, J. S., Matsuda, Y. and Ishimoto, A. (2000). Biochemical characterization of the Drosophila axin protein. *FEBS Lett.* **474**, 189-194.

Yost, C., Torres, M., Miller, J. R., Huang, E., Kimelman, D. and Moon, R. T. (1996). The axis-inducing activity, stability, and subcellular distribution of beta-catenin is regulated in Xenopus embryos by glycogen synthase kinase 3. *Genes Dev.* **10**, 1443-1454.

Zecca, M., Basler, K. and Struhl, G. (1996). Direct and long-range action of a wingless morphogen gradient. *Cell* **87**, 833-844.